Lawrence Berkeley National Laboratory
Lawrence Berkeley National Laboratory

Title
LASER INDUCED FLUORESCENCE OF TRAPPED MOLECULAR IONS

Permalink
https://escholarship.org/uc/item/82q5d2vm

Author
Winn, J.S.

Publication Date
1980-10-01

Peer reviewed

eScholarship.org Powered by the California Digital Library
University of California

LBL-12002
CONF-8009131--1

Lawrence Berkeley Laboratory
UNIVERSITY OF CALIFORNIA

Materials & Molecular Research Division

Invited lecture presented at the NATO International Advanced Study Institute, "Molecular Ions: Geometric and Electronic Structures", Kos, Greece, September 30-October 10, 1980

LASER INDUCED FLUORESCENCE OF TRAPPED MOLECULAR IONS

John S. Winn

October 1980

MASTER

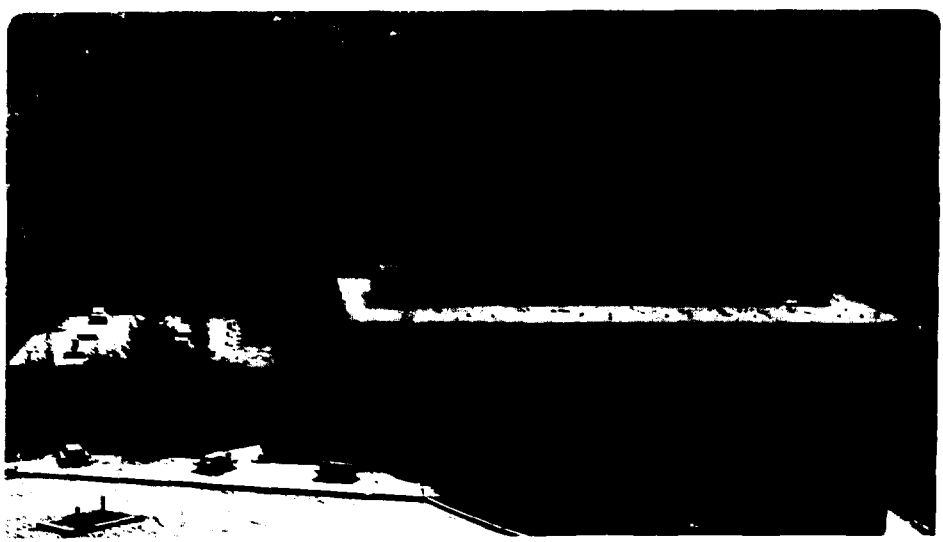

Prepared for the U.S. Department of Energy under Contract W-7405-ENG-48

Introduction

Laser induced fluoresence (LIF) spectra (laser excitation spectra) are conceptually among the most simple spectra to obtain. One need only confine a gaseous sample in a suitable container, direct a laser along one axis of the container, and monitor the sample's fluorescence at a right angle to the laser beam. As the laser wavelength is changed, the changes in fluorescence intensity map the absorption spectrum of the sample. (More precisely, only absorption to states which have a significant radiative decay component are monitored.) For ion spectroscopy, one could benefit in many ways by such an experiment. Most optical ion spectra have been observed by emission techniques, and, aside from the problems of spectral analysis, discharge emission methods often produce the spectra of many species, some of which may be unknown or uncertain. Implicit in the description of LIF given above is certainty as to the chemical identity of the carrier of the spectrum.

This article describes a method by which the simplifying aspects of LIF can be extended to molecular ions (albeit with a considerable increase in experimental complexity over that necessary for stable neutral molecules). Briefly, we use a quadrupole ion trap to store and spatially confine ions. The trap is mass-selective, affording

species identification over a large mass range. The laser is pulsed, allowing time-resolved studies of various types. This experiment has been developed over several years in collaboration with Prof. Bruce Mahan, Dr. Fred Grieman, and Mr. Tony O'Keefe. The article is divided into two main sections. The first describes the apparatus in some detail, and the second gives selected results demonstrating the types of measurements which are made possible. Further details of the apparatus can be found elsewhere.[1]

Experimental Method

A. Ion Trap

The experimental apparatus is based on the ability to confine a sufficient number of molecular ions in a electric field of suitable geometry. There are many types of trap designs discussed in the literature.[2] Before discussing the design we have chosen, a few comments are in order on the desirability of using a trap over other ion sources.

One alternative technique, exemplified by the work of Carrington[3], is to use an ion beam source. A beam has the advantages of spatial localization and velocity control, and high resolution spectra can result from various methods which reduce the Doppler width of the beam-laser interaction. A decided disadvantage is the relatively low number density

of ions in a focussed, mass selected ion beam. For example, a typical mass 40 ion beam with a cross-sectional area of 0.04 cm^2, a laboratory energy of 100 eV, and an ion current of 1 namp has a ion density of 7×10^4 cm^{-3}. Of these 7×10^4 ions, a crossed ion-laser beam interaction geometry would irradiate only ~3000 ions per cm of irradiated ion beam length, assuming a 2x2 mm ion beam cross-section. By the time one multiplies this figure by a typical population distribution for what are generally rather hot ions, the number of ions in any given quantum state has fallen below detectability by LIF.

One can use discharge flow methods, as demonstrated by Miller and coworkers.[4] The ion density is considerably greater and the ions can be equilibrated to the temperature of the carrier gas. This temperature can be made significantly lower than ambient. One potential drawback is the lack of ionized species isolation and identification which a mass spectrometer allows. The identification of the carrier of a spectrum is not automatic in a discharge flow where perhaps many types of ions or radicals are present.

The ion trap therefore offers the following experimental conditions. The ion density can be made sufficiently large ($\geq 10^6$ cm^{-3}) for a reasonable detection probability. The trapped ion mass can be varied, allowing unambiguous

chemical identification. The trap can be operated at sufficiently low pressures so that ions can be confined in a collision-free environment for long times (long compared to fluorescence decay times and, generally, for times which are limited by the ion-neutral collision rate). From the very nature of collision-free trapping, one gains the added benefit that the ion state distribution reflects the nascent distribution resulting from the chosen ionization method. For favorable systems, one can trap ions for times on the order of many collision periods. One can in this way study inelastic collision processes and perhaps follow the course of reactive ion-molecule collisions. On the negative side, the rather high velocity and chaotic motion characteristic of trapped ions limits the spectral resolution. Progress has been made toward reducing the velocity spread of trapped ions; the rather spectacular results[5] obtained by laser cooling of atomic ions is one potentially useful method .

The ion trap we use is cylindrical in geomety. Design criteria for such traps have appeared in the literature.[6] The cylindrical design was chosen over a more conventional hyperbolic design[2] primarily to allow the various apertures needed for light entrance and exit to be cut into the trap without seriously disturbing the electric fields.

A cut-away assembly drawing, showing more than the trap itself, is shown in Fig.1. The trap itself consists of two end, or cap, electrodes which are electrically grounded (2 and 5 in Fig.1) and a cylindrical center electrode (denoted 3 in Fig.1). Two dimensions determine the trap geometry: the cap-to-cap spacing, $2z_1$, and the radius of the cylindrical center electrode, r_1. By changing the removeable cap electrode cones (horizontally shaded portions of 2 and 5 in Fig.1), we can alter the z_1 to r_1 ratio. In our design, r_1 = 1.43 cm, and cap electrode cones are available to permit $z_1 = r_1$ or $2z_1^2 = r_1^2$. The latter geometry closely approximates the ideal hyperbolic case.[6]

Trapping is achieved by applying a potential of the form $U + V\cos\omega t$ to the center electrode. U is a constant potential; V is the amplitude of an r.f. potential of frequency ω. By changing the ratio U/V one changes the range of masses which can be trapped. By changing the magnitudes of U and V while maintaining a constant ratio, one changes the center of this range of masses. Thus one can trap all ions, ions of only one mass, or ions of neighboring masses. In our design, the maximum mass we can trap is ~100 amu and the maximum useable resolution is $m/\Delta m \sim 40$.

The other components of the trap region shown in Fig.1 are described briefly below. Ionization is attained by

electron bombardment from an electron gun (13). The gun uses a thoriated W filament and is tightly enclosed to reduce scattered filament light. The electron current (~50 μamp maximum) is monitored by a small Faraday cup (4). Laser light passes through the trap in a direction perpendicular to the plane of Fig.1. How this is done is described in greater detail below. Fluorescence passes through the planar end electrodes, which are wire mesh. If emitted downwards, the light is reflected back up by the metallic spherical mirror (9). Upward fluorescence is gathered by a Fresnel lens (17), directed through a quartz window (14) through the vacuum and onto the photocathode of the detection photomultiplier (not shown in Fig.1).

To determine the ion density, a magnetic strip electron multiplier (15) is located beneath the trap. A magnetic shield (10) isolates this device from the trap region. By applying appropriate voltages to the trap, mirror, and associated plates (6, 8, and a Cu insert in 10), ions are pulsed out of the trap and detected. It is vital that ions are pulsed out of the trap at the same point in the r.f. cycle of the trap in order to obtain reproduceable measures of the ion density.

Ancillary pieces shown in Fig.1 include the multiplier mount (11), a Teflon insulator (7), one of the height adjustment assemblies (1 and 12) and the locating pin (16) which

precisely repositions the trap assembly into the vacuum chamber. Note also that ceramic balls are used to position, insulate, and space the trap electrodes.

An assembly diagram of the remainder of the trap chamber is shown in Fig.2. The laser beam entry and exit arms are shown in relation to the trap itself. Extensive light baffles are used to reduce scattered light, as are (occasionally) band pass filters before the photomultiplier.

B. Optical System

The laser is a Molectron nitrogen laser pumped dye laser. Due to Doppler motion, the laser bandwidth need be no less than ~0.6 cm^{-1}. The laser pulse is 5 to 10 nsec in duration with an energy of 50 to 500 μJ/pulse. Laser power on a shot-to-shot basis is monitored with a photodiode. The laser repetition rate is usually kept at its maximum of 40 Hz. Laser wavelength is monitored optogalvanically.[7] A hollow cathode discharge in Ne is mounted past the exit window. Impedence changes in the discharge due to laser excitation of excited Ne atoms is monitored as the laser wavelength is changed. The numerous Ne* transitions throughout the visible region of the spectrum provide calibration markers.

Fluorescence is collected by the lens and mirror system mentioned above. They have a geometric collection

efficiency of 10%. The detector is a cooled photomultiplier tube operated in a photon-counting mode.

C. Experimental Timing

Since the laser is pulsed and the ions are stored for, at most, some small fraction of a second, the entire experiment is continuously cycled under computer control. A typical cycle follows. The electron gun is fired for about 2 msec. Mass selection and fluorescence decay (from electron bombardment) is allowed to occur for about 0.1 to 1.0 msec. The laser is fired and its power recorded. After a second delay of up to several μsec (but more typically tens of nsec), the gain of the photomultiplier tube is switched from a low to a useable, high value, and fluorescence counts are accumulated. Ions are then pulsed from the trap and their density recorded. The optogalvanic signal is measured, and one cycle is ended. This cycle is repeated at a given wavelength for a predetermined number of laser shots. The wavelength is then advanced a preset amount, and a new set of cycles is initiated. The relevant signal is the raw fluorescence normalized to laser power and ion density recorded as a function of the laser frequency. Spectra are stored on disks for later manipulation and display by the computer.

Ten nsec, the laser pulse duration time, is generally a brief period in the radiative lifetime of an electronically excited molecule. We can thus measure radiative decay by changing the experimental setup slightly. We keep the laser fixed at one wavelength in coincidence with a previously assigned feature in the spectrum. Then the fluorescence is monitored after each laser shot by a fast multichannel scaler (minimum channel width = 10 nsec). Data are accumulated for hundreds to many thousands of laser shots. Background radiation is subtracted from this signal by detuning the laser and repeating the measurement. A normal single exponential fluorescence decay curve results.

D. Other Experimental Remarks

We typically fill the vacuum chamber to a pressure $\sim 10^{-5}$ torr with the necessary parent neutral ion. Primary ions are easily produced. Fragment ions, however, are subject to large, and generally unknown, repulsive kicks when they are formed. The laboratory kinetic energy gained by these kicks depend on fragment masses and details of the dissociation dynamics. One possible result is an inability to stabilize high velocity fragments by the trap fields themselves. We have successfully found the CH^+ fragment from both CH_4 and C_2H_2 ionization, as discussed below, but we have not yet explored the possible difficulties of

trapping fragment ions in general.

Trapped ions zip around the trap with high velocity. As a result, the addition of a buffer gas is likely to heat ions rather than collisionally cool them. Whether this is an advantage or a disadvantage depends on one's point of view. Likewise, the initial state distribution of the ions depends on the molecule and the energy distribution of the ionizing electrons. Electrons are injected into the trap, and they undergo energy changes which are difficult to control. As a result, more detailed studies of the ionization process itself could be done with, for instance, a photoionization source, but only at a considerable loss in ion density.

Experimental Results

A. Diatomic LIF Spectra

Given the limitations in spectral resolution of our experiment, the relatively sparse level structure of light diatomic ions becomes the most advantageous to explore. Our spectra of the fragment ions CH^+ and CD^+ will be described briefly here as examples of the types of spectra one can expect. Further details of these spectra can be found elsewhere.[8]

The best known and most important band system of CH^+ is the $A\ ^1\Pi \leftarrow X\ ^1\Sigma^+$ system. This system has been characterized

in emission[9] and is of importance to the astrophysical problem of CH^+ formation via radiative association[10]. We have produced CH^+ and CD^+ from CH_4, C_2H_2, and the perdeuterated compounds. The (0,0) and (2,1) bands have been measured, and an example (the CH^+(0,0) band) is shown in Fig. 3. The spectrum is easily assigned, but the rotational distribution indicated significantly hotter ions than are seen in emission. Emission spectra followed the R branch out to the R(7) line; we have seen lines out to R(21). While we gain in quantity of information, we are, as Fig. 3 indicated, limited in resolution to a few tenths of a wavenumber. In this case, the gain in quantity was the more desirable outcome. We found that the new lines at high J could not be fit by the existing molecular constants. We therefore refit our CH^+ and CD^+ lines to a new set of constants which are given in Table I.

We have also observed known bands in N_2^+ and CO^+. While we do not add new spectroscopic information to that already known for these molecules, our data on them are of interest for other reasons, as discussed below.

B. Polyatomic LIF Spectra

We have observed spectra for two polyatomic ions in detail, $BrCN^+$ and 1,3,5-trifluorobenzene cation. Spectra

have also been found for H_2S^+ and $ClCN^+$, but these have not been examined in great detail.

For $BrCN^+$, the B $^2\Pi$ ← X $^2\Pi$ system extending from 20 000 to 24 500 cm^{-1} was investigated.[11] The ions were found to be internally hot, and rotational resolution was impossible. However, a vibrational progression, assigned to the ν_1 mode (primarily C-Br stretch) of the B state was observed. The frequency was found to 441±18 cm^{-1}. This is an average band spacing and does not properly account for anharmonicities, nor are observed irregularities in the band-to-band spacings fully explained. Each band is split by the spin-orbit interactions of each state. We find a difference in the spin-orbit constants to be A"-A' = 224±43 cm^{-1}.

$BrCN^+$ is not the ideal ion to study by this method. Not only are the ions hot and the levels closely spaced, but overlapped sequence bands and Fermi interaction (between ν_2" = 290 cm^{-1} and ν_1' = 441 cm^{-1} or ν_1" = 509 cm^{-1}) cause nonsystematic spacings and intensity irregularities.

To test our trap near the limit of its mass range, we investigated the B A_2" ← X E" band system of the 1,3,5-trifluorobenzene cation, which has a mass of 132 amu. We were able to trap the ion, but with a mass resolution of only 15. This value is purely the result of the particular power supply we used to operate the trap. Thus, we may have co-trapped fragment ions along with the desired parent, but our

spectra[1] agreed well with those obtained by others.[4,12] In general, the many bands we observed were in good agreement with those of previous assignments, but we lacked the resolution (due to the ion temperature) needed to provide the more detailed interpretations of Miller and Bondybey, who worked with colder gaseous ions and with matrix isolated ions.

C. Radiative Lifetimes

We have tested the ability of our apparatus to record rediative lifetimes over a considerable range of values. The strong N_2^+ first negative system, $B\ ^2\Sigma_u^+ \rightarrow X\ ^2\Sigma_g^+$, is characterized by a 60 nsec radiative lifetime, which we measure without difficulty. This value is not constant throughout the spectra, however. Perturbations by the longer-lived $A\ ^2\Pi_u$ state are known[13], and perturbations by an unknown $^4\Sigma_u^+$ state have been suspected.[14] Our N_2^+ spectra extend to high rotational quantum number, N, and we plan a systematic search for lifetime perturbations throughout the spectra.[15]

At the long end of the radiative lifetime scale, we have observed and verified the 3.25 μsec lifetime of the CO^+ $A\ ^2\Pi \rightarrow X\ ^2\Sigma^+$ ($v'=2$) band. The lifetime of CH^+ is known to be intermediate to these extremes. Other measurements have relied on fast electron pulse excitation to initiate the experiment. As Erman[16] has shown, these measurements can be systematically low due to the rapid spatial dissipation of ions from the

viewing region due to ion-ion repulsive forces. His result, 630 nsec, was the largest reported experimental value, yet it is below the theoretical range (660 - 800 nsec) predicted by the ab initio calculations of Yoshimine, Green, and Thaddeus.[17] Our method does not suffer from such a systematic error. Therefore, we measured the lifetime of CH^+ ($A\ ^1\Pi$) in order to compare to the electron excitation value and the ab initio value. Our result[8] was 815±25 nsec, in good agreement with the upper range of the theoretical value and clearly at odds with the electron excitation value.

D. Ion State Distributions

The collision-free nature of the trap affords us the opportunity to probe the nascent internal state distribution of ionized molecules and fragments. Of course, we use the term "nascent" to mean the distribution in the ground or optically metastable states which result after radiatve cascade from the truly nascent excited states which may be formed. Emission spectra, when recorded under single collision conditions, yield these excited state distributions. In a more practical vein, however, the ground or metastable state distributions we observe are of considerable importance to experiments which use ions after fast decay processes have occured, but before thermalizing collisions (or infrared

fluorescence) have otherwise altered the energy distribution. Inelastic and reactive scattering experiments with ion beams are clear examples of such a situation.

Ionization of CO is one case we have begun to study. The comet-tail system, $A\ ^2\Pi - X\ ^2\Sigma^+$, mentioned above in regards to lifetime measurements, is a useful band system to use in probing the X state internal energy distribution. We produce CO^+ by bombardment with electrons of roughly 150 eV energy. Cross sections for excitation to levels in the A state have been measured,[18] and high vibrational levels of the A state are known to be populated with significant probability. Moreover, the A→X Franck-Condon factors are known, and they indicate that the X state will become vibrationally h[illegible]s a result of A→X decay. The X state is not expe[illegible] to be formed in high vibrational levels as a result of [illegible]imary ionization from room temperature CO.

Fig.4 verifies this prediction. Portions of the (7,7) and (4,5) LIF bands are shown. Population in X (v" = 7 or 5) is essentially all due to cascade from the A state. We are currently measuring other band intensities, from which we expect to obtain a very complete picture of the ionization of CO.

A second example involves the fragment ions CH^+ and CD^+. As noted above, we find[8] these ions to be rather hot; we estimate a rotational temperature near 3000 K and a vibrational temperature near 5500 K. Somewhat more remarkable is the

observation that these temperatures are obtained whether we use CH_4 or C_2H_2 as the parent gas.

E. Collisional Energy Transfer and Product State Analysis

The translational motion of trapped ions is well above the ambient temperature of the parent gas. A temperature of ~4000 K is typical.[8,19] If we produce N_2^+, for instance, we find[1] a rotational distribution in the ground state characterized by a temperature of 300±25 K. This result is obtained following a 1 msec ionization period on pure N_2 at a pressure of ~5 x 10^{-6}torr. (Recall that under these conditions, the ion-neutral collision rate is ~1 $msec^{-1}$.) We can easily follow the consequences of a few collisions by raising the N_2 pressure, by waiting for longer times before we fire the laser, and/or by adding a non-trapped, chemically inert buffer gas at a higher concentration. For example, a spectrum of N_2^+ produced by 1 msec ionization of a mixture of Kr (3 x 10^{-4}torr) and N_2 (5 x 10^{-5}torr) shows considerable collision induced rotational heating. The rotational temperature rises to 585±15 K. (An increase in vibrational temperature is also apparent from the spectrum, but the effect is more difficult to make quantitative.)

This experiment shows two important facts. First, ions can be confined for times long enough that the consequences of several collisions can be probed, and secondly, these

consequences can be measured. For reactive collisions, we envision, but have not yet attempted, an experiment of the following type. A mixture of a heavy gas (such as N_2) and a light gas (such as H_2) with the light gas in excess is admitted to the trap. The mass resolution is adjusted to yield trapping of the heavy primary ion and the only slightly heavier product ion which would result from a reactive collision (such as N_2H^+). Many exothermic ion-molecule reactions are known to proceed at virtually every collision. We have constrained the reaction dynamics by a choice of masses which insures that the product will not receive a large translational impulse on reaction. We therefore co-trap the primary reactant ion and the ion-molecule reaction product which we investigate by LIF. As the alert reader has no doubt noticed, the principle drawback of this scheme is the general lack of spectroscopic data on most product ions which are otherwise suitable for such an experiment.

Summary

This article has given an overview of the experimental opportunities afforded by studying the laser induced fluorescence spectra of molecular ions confined in a mass selective ion trap. The advantages include species identification, collision control ranging from none to several collisions, timed measurements leading to radiative lifetimes, delayed

excitation leading to the study of collisional alteration of the nascent ion state distribution, and the spectroscopic advantages LIF spectra give to complement emission spectra. The primary disadvantages are the large Doppler widths of spectral lines and, as always, an ion density that borders on the low end of usefulness.

Acknowledgement

This research was supported by the U.S. Department of Energy, Office of Basic Energy Sciences, Division of Chemical Sicences under Contract No. W-7405-Eng-48. The radiative lifetime of CH^+ and the spectrum of CO^+ shown in Fig. 4 were obtained using a Nd:YAG pumped dye laser supplied by the San Francisco Laser Center, supported by a grant to the University of California and Stanford University from the National Science Foundation under grant CHE79-16250.

References

1. T.J. Grieman, "Laser Induced Fluorescence of Trapped Molecular Ions", Lawrence Berkeley Laboratory Report LBL-10021, (1979) (Ph.D. Thesis).
2. P.H. Dawson and N.R. Whetton, Adv. Electronics and Electron Phys., 27, 59 (1969); H.G. Dehmelt, Adv. At. Mol. Phys. 3, 53 (1967).
3. A. Carrington, D.R.J. Milverton, P.G. Roberts, and P.J. Sarre, J. Chem. Phys. 68, 5659 (1979).
4. T.A. Miller, V.E. Bondybey, and J.H. English, J. Chem. Phys. 70, 2919 (1979).
5. D.J. Wineland, J.C. Bergquist, W.M. Itano, and R.E. Drullinger, Opt. Lett. 5, 245 (1980).
6. M. Benalin and C. Audoin, Int. J. Mass. Spec. Ion Phys. 11, 421 (1973); R.F. Bonner, J.E. Fulford, and R.E. March, Int. J. Mass Spec. Ion Phys. 24, 255 (1977).
7. D.S. King and P.K. Schenck, Laser Focus, March, 1978, p. 60.
8. F.J. Grieman, B.H. Mahan and A. O'Keefe, J. Chem. Phys. 72, 4246 (1980); F.J. Grieman, B.H. Mahan, A. O'Keefe, and J.S. Winn, (to appear in Discussions of the Faraday Soc. No. 71, 1981).
9. A.E. Douglas and G. Herzberg, Can. J. Res. 20, 71 (1942); A.E. Douglas and J.R. Morton, Ap. J. 131, 1 (1960).
10. A. Dalgarno, in Atomic Processes and Applications, ed. by P.G. Burke and B.L. Moiseiwitsch (North Holland, Amsterdam, 1976), p. 110.
11. F.J. Grieman, B.H. Mahan, and A. O'Keefe, J. Chem. Phys. (in press).
12. V.E. Bondybey, T.A. Miller, and J.H. English, J. Chem. Phys. 71, 1088 (1979) and references therein.

13. R.A. Gottscho, R.W. Field, K.A. Dick and W. Benesch, J. Mol. Spectrosc. 74, 435 (1979).
14. J. Dufay and O. Nedelec, C.R. Acad. Sci. Ser. B 285, 173 (1977).
15. A. O'Keefe and J.S. Winn (unpublished results).
16. P. Erman, Ap. J. 213, 289 (1977).
17. M. Yoshimine, S. Green and P. Thaddeus, Ap. J. 183, 899 (1973).
18. R.F. Holland and W.G. Maier, II, J. Chem. Phys. 56, 5229 (1972); J.F.M. Aarts and F.J. DeHeer, Physica 49, 425 (1970); J.M. Ajello, J. Chem. Phys. 55, 3158 (1971).
19. R.D. Knight and M.H. Prior, J. Appl. Phys. 50, 3044 (1979).

Table I. Molecular constants for CH^+ and CD^+. Energies are in cm^{-1} units.

CH^+ (0,0) band ν_{00} = 23596.81(01)*			
$X\ ^1\Sigma^+$		$A\ ^1\Pi$	
B_0	13.9303(40)	B_0^{RP}	11.4532(37)
D_0	$1.373(11) \times 10^{-3}$	B_0^Q	11.4169(41)
		D_0^{RP}	$2.050(9) \times 10^{-3}$
		D_0^Q	$2.049(11) \times 10^{-3}$
		q_0	0.038

CD^+ (0,0) band ν_{00} = 23747.71(1)			
B_0	7.627(20)	B_0^{RP}	6.285(20)
D_0	$1.06(15) \times 10^{-3}$	B_0^Q	6.280(21)
H_0	$1.55(35) \times 10^{-6}$	D_0^{RP}	$1.08(14) \times 10^{-3}$
		D_0^Q	$1.16(16) \times 10^{-3}$
		H_0^{RP}	$1.12(29) \times 10^{-6}$
		H_0^Q	$1.41(37) \times 10^{-6}$
		q_0	0.016

(Table I - continued)

CD^+ (2,1) band

ν_{21} = 24095.08(1)

B_1	7.416(46)	B_2^{RP}	5.492(44)
D_1	1.25(56) x 10^{-3}	B_2^Q	5.479(49)
H_1	4.5(2.0) x 10^{-6}	D_2^{RP}	8.8(4.8) x 10^{-4}
		D_2^Q	7.1(6.2) x 10^{-4}
		H_2^{RP}	2.5(1.5) x 10^{-6}
		H_2^Q	1.2(2.2) x 10^{-6}
		q_2	0.014

*Numbers in parentheses represent a one standard deviation uncertainty in the last digits of each constant.

Figure Captions

Fig. 1 Cross sectional drawing of the ion trap assembly. Numbered items are identified in the text.

Fig. 2 Assembly drawing of the vacuum chamber with the trap assembly in place. The photomultiplier detector mounts onto the ion trap apparatus flange and views the trap through the quartz window.

Fig. 3 LIF spectrum of the (0,0) band of the CH^+ A-X system. Features from the (2,1) band (such as Q_9) appear weakly in this spectral region.

Fig. 4 LIF spectrum of the (7,7) and (4,5) bands of the CO^+ A-X system.

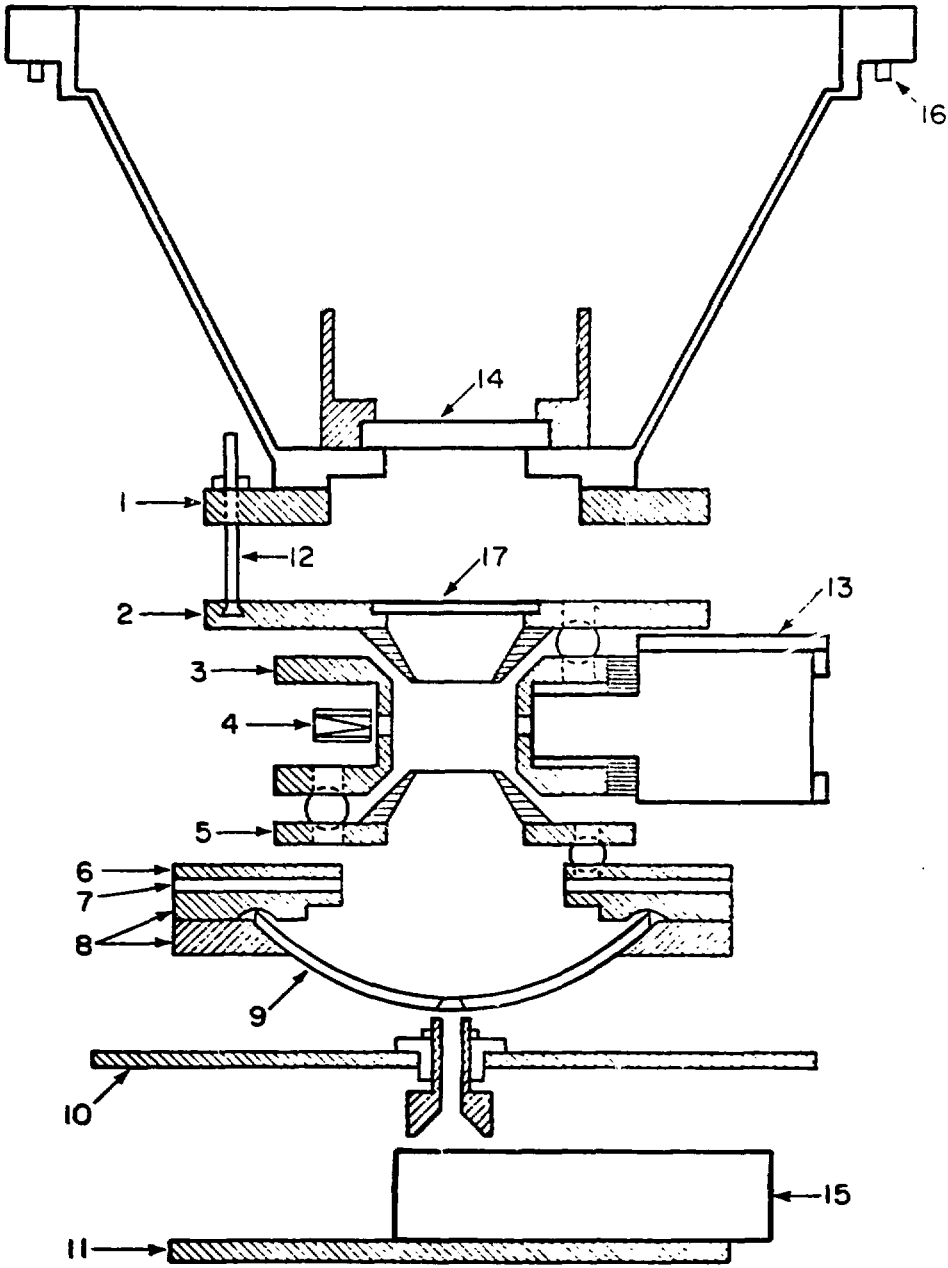

Figure 1
XBL-798-11091

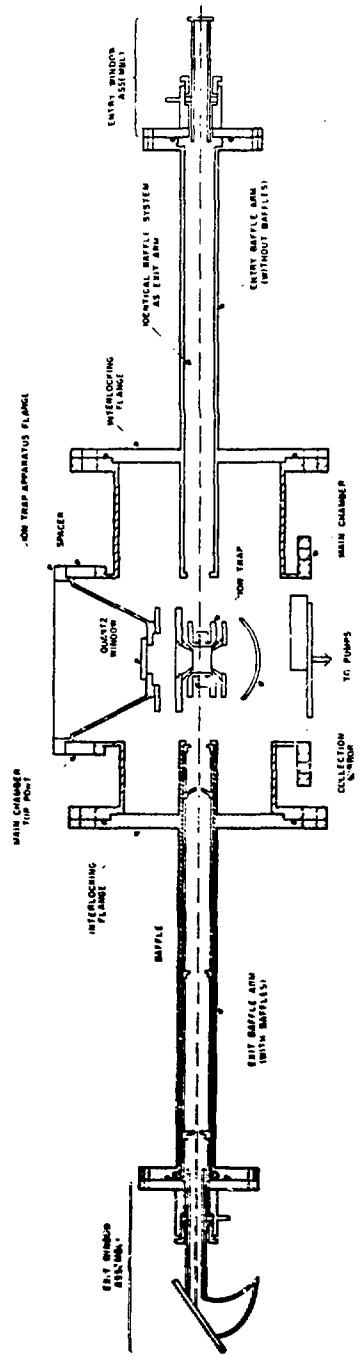

Figure 2
XBL-798-11093

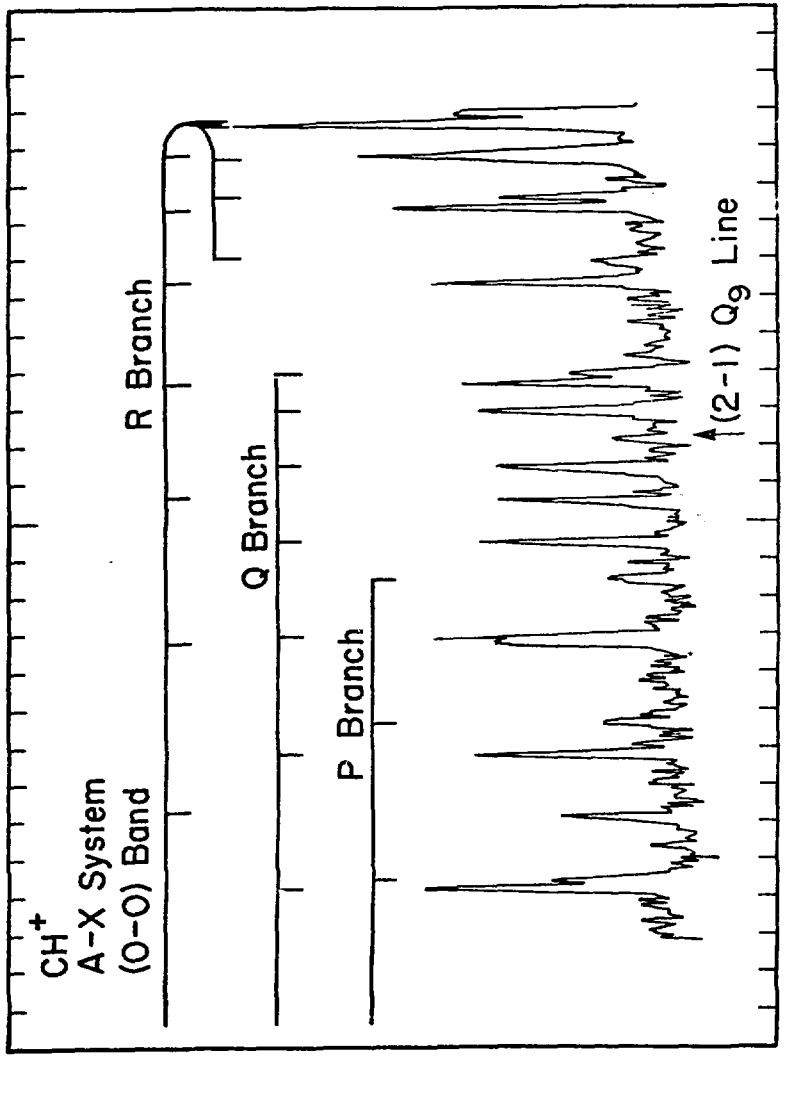

XBL 808-11411

Figure 3

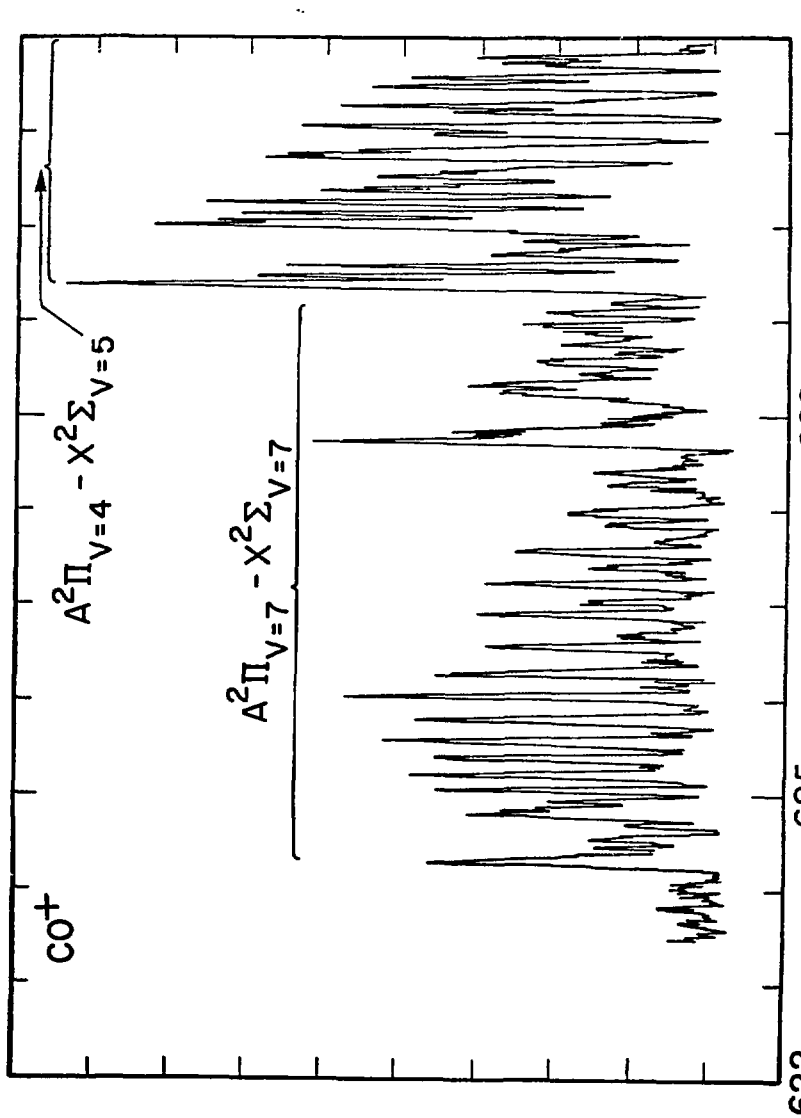

XBL 808-11412

Figure 4